Supplementary Information (SI) for Inorganic Chemistry Frontiers.

Multi-color afterglow from amorphous hybrid perovskites for flexible programmable composites with heterostructure

Liwen Kang, ‡ Jinyu Xu, ‡ Junyan Wu, Qidan Ling and Zhenghuan Lin**

Fujian Key Laboratory of Polymer Materials, College of Chemistry and Materials Science, Fujian Normal University, Fuzhou 350007, China

E-mail: wu-jy@fjnu.edu.cn and zhlin@fjnu.edu.cn

‡ *These authors contributed equally to this work*

Experimental Section

General Methods

Prompt photoluminescence spectra were obtained at the room temperature using an Edinburgh FS5 spectrofluorometer with a xenon arc lamp (Xe900). Time-resolved photoluminescence decay curves and delay spectra were obtained using a FLS920 fluorescence spectrometer equipped with a microsecond flash-lamp (μF900), and a nanosecond hydrogen flash-lamp (nF920). The single-crystal structure was analyzed by German Bruker Technologies SMART APEX II single-crystal diffractometer quipped with graphite monochromated Mo Kα radiation. The crystalline structure of powder samples was determined by PXRD using a PANalytical X-ray diffractometer (X'Pert3 Powder) with Cu Kα radiation (λ = 1.54178 Å) with a step size of 5o min−1. UV–visible absorption spectra were measured using a Shimadzu UV2600 spectrophotometer. Fourier Transform Infrared Spectroscopy (FTIR) was carried out on Thermo-Nocilet IS50 equipped with a mini X-ray tube-2 (Amptek, Inc., Ag target). Thermogravimetric analysis (TGA) data were obtained by Mettler thermogravimeter, and the heating rate was 10 oC. Differential scanning calorimetry (DSC) data were obtained by METTLER DSC3 differential scanning calorimeter. Scanning Electron Microscopy (SEM) and Energy Dispersive Spectrometer (EDS) photos are obtained from HITACHI Regulus Field Emission Scanning Electron Microscope. Raman spectra were collected using a DXR2xi Raman Imaging Microscope. The photos under polarized light was taken by LV100N, a Japanese Nikon polarizing microscope.

Chemicals and Materials

N-aminoethyl piperazine (AEPZ), cadmium chloride ($CdCl_2$), manganese chloride ($MnCl_2$) and rhodamine B (RB) were purchased from Tansoole. The commercial polylactic acid (PLA) 4032D was purchased from Nature Works (Nebraska, America). HCl (36 wt%) and other organic solvents were purchased from Sinopharm. All chemicals were obtained from commercial suppliers and used directly in the experiments without further purification unless otherwise stated.

Theoretical Calculations

On the basis of Gaussian 09 D.01 program package, time-dependent density functional theory (TD-DFT) were employed for all calculations with cam-b3lyp functional and a mixed basic set where main group elements and transition metal Cd were described with 6-311g(d,p) and Stuttgart pseudopotential (sdd), respectively. Wavefunction analysis were executed using

Multiwfn 3.8(dev) that updated at 2024.07.29. Visualization of the electrons and holes was achieved using the VMD1.9.3 software.[1]

Synthesis of AC1

AEPZ (1.5 mmol, 193.8 mg), $CdCl_2$ (0.5 mmol, 91.66 mg) and HCl (12 M, 9 mL) were put into a 20 ml glass bottle, and heated at 120 °C until the solid was completely dissolved, and then gradually cooled to room temperature and stood for one week. The AC1 was obtained in solid after filtration and drying at 60 °C overnight.

Synthesis of AC2

AEPZ (0.5 mmol, 64.6 mg), $CdCl_2$ (2 mmol, 366.6 mg) and HCl (12 M, 9 mL) were put into a 20 ml glass bottle, and heated at 120 °C until the solid was completely dissolved, and then gradually cooled to room temperature and stood for one week. The AC2 was obtained in solid after filtration and drying at 60 °C overnight.

Synthesis of AC1-A or AC2-A

The amorphous AC1-A and AC2-A can be obtained by heating the AC1 and AC2 crystals to 248 °C and 240 °C in a circular glass mold and then rapidly cooling them to below 10 °C, respectively.

Synthesis of AC3-A

In the process of synthesizing AC2 crystal, dopants of RB (23.95 mg, 0.05 mmol) was added to obtain a crystal which was heated to 240 °C in a circular glass mold and then rapidly cooling them to below 10 °C to give AC3-A.

Synthesis of AC4-A

In the process of synthesizing AC2 crystal, dopants of $MnCl_2$ (25.17 mg, 0.2 mmol) was added to obtain a crystal which was heated to 240 °C in a circular glass mold and then rapidly cooling them to below 10 °C to give AC4-A.

Synthesis of AC-A@PLA

The mixture of AC crystal and PLA was heated to 240 °C until melted. After crystal and PLA were mixed evenly, they were drawn in the air with tweezers to give AC-A@PLA filaments.

Density calculation method of AC-A

Firstly, the mass of AC-A is weighed by electronic balance, then the AC-A is put into a measuring cylinder filled with acetone, and the volume of the material is calculated according to the rising height of the solvent. Finally, the density of AC-A is calculated by formula $\rho(g/cm^3) = m(g)/v(cm^3)$.

Table S1 Crystal data and structure refinement for AC1 and AC2.

Crystal	AC1	AC2
Dimension	0D	1D
Formula	$C_{12}H_{36}CdCl_8N_6$	$C_6H_{24}Cd_2Cl_7N_3O_3$
formula weight	330.23	659.23
Shape	Bulk	Flake
crystal system	monoclinic	triclinic
space group	P 2_1/c	P -1
a (Å)	9.9703(2)	9.1796(2)
b (Å)	10.9517(2)	9.7022(3)
c (Å)	12.0652(3)	12.9682(3)
α(deg)	90	83.346(2)
β(deg)	108.645(2)	72.142(2)
γ(deg)	90	66.040(2)
V (Å3)	1248.28(5)	1004.55(5)
Z	2	2
Dcalcd.(g/cm3)	1.757	2.179
F(000)	668	640
R (int)	0.0756	0.0465(3825)
GOF on F2	1.074	1.060
R1[I > 2σ(I)]	0.0491	0.0465
wR2 [I>2σ(I)]	0.1382	0.1293
R1 (all data)	0.0498	0.0472
wR2 (all data)	0.1396	0.1304
CCDC number	2418027	2418028

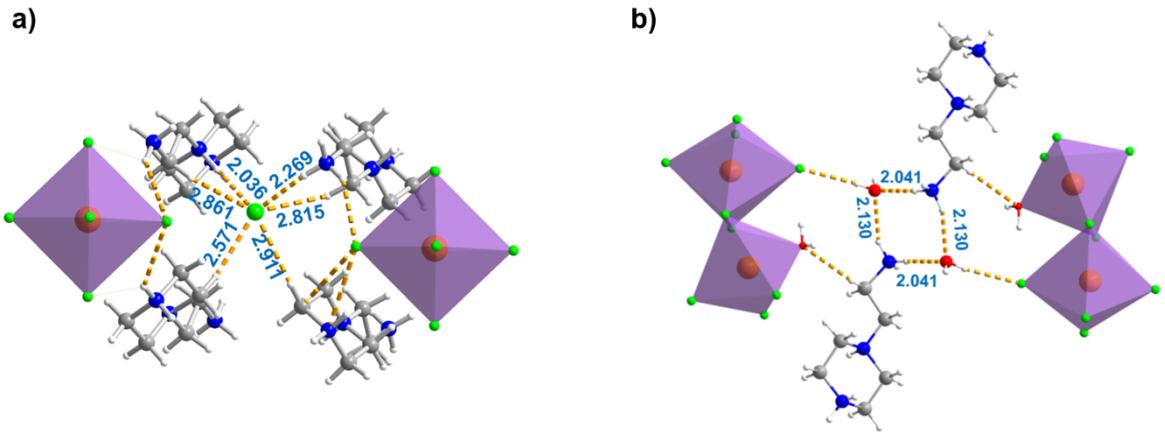

Fig. S1 Arrangement of organic molecules in crystal structures of a) AC1 and b) AC2.

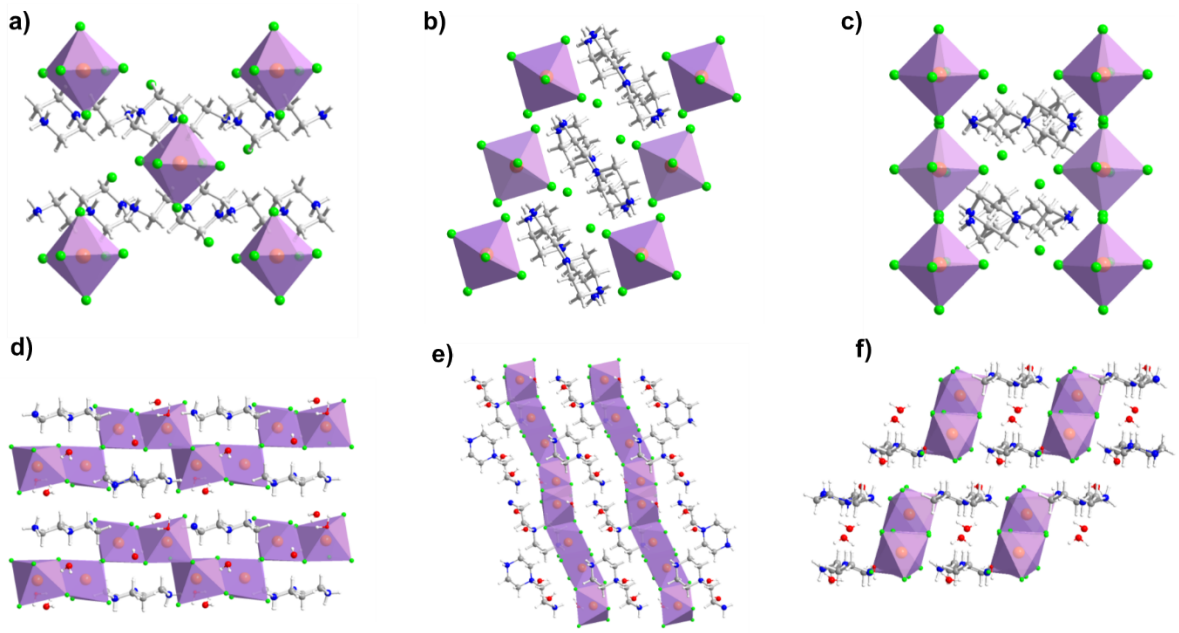

Fig. S2 Crystal packing structures of a-c) AC1, d-f) AC2 with different orientations.

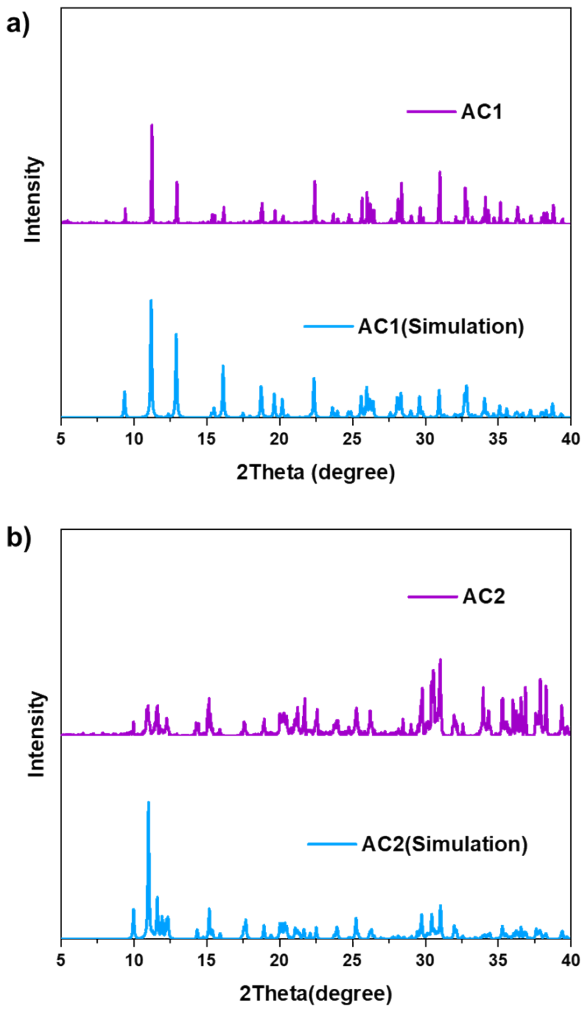

Fig. S3 Experimental and simulated PXRD patterns of a) AC1and b) AC2.

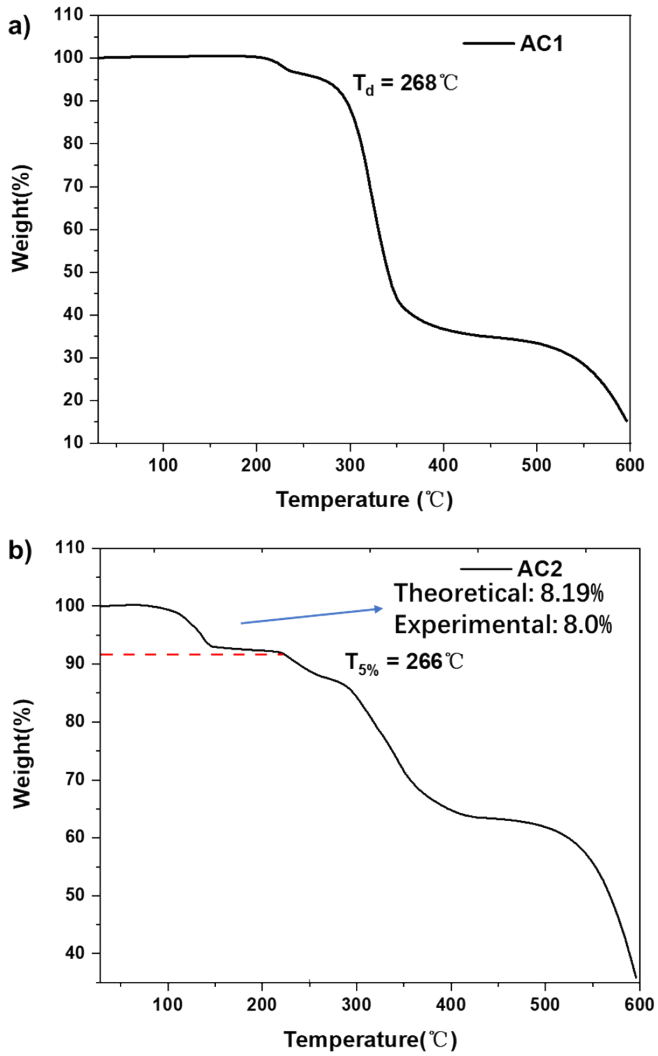

Fig. S4 Thermogravimetric analysis of a) AC1 and b) AC2.

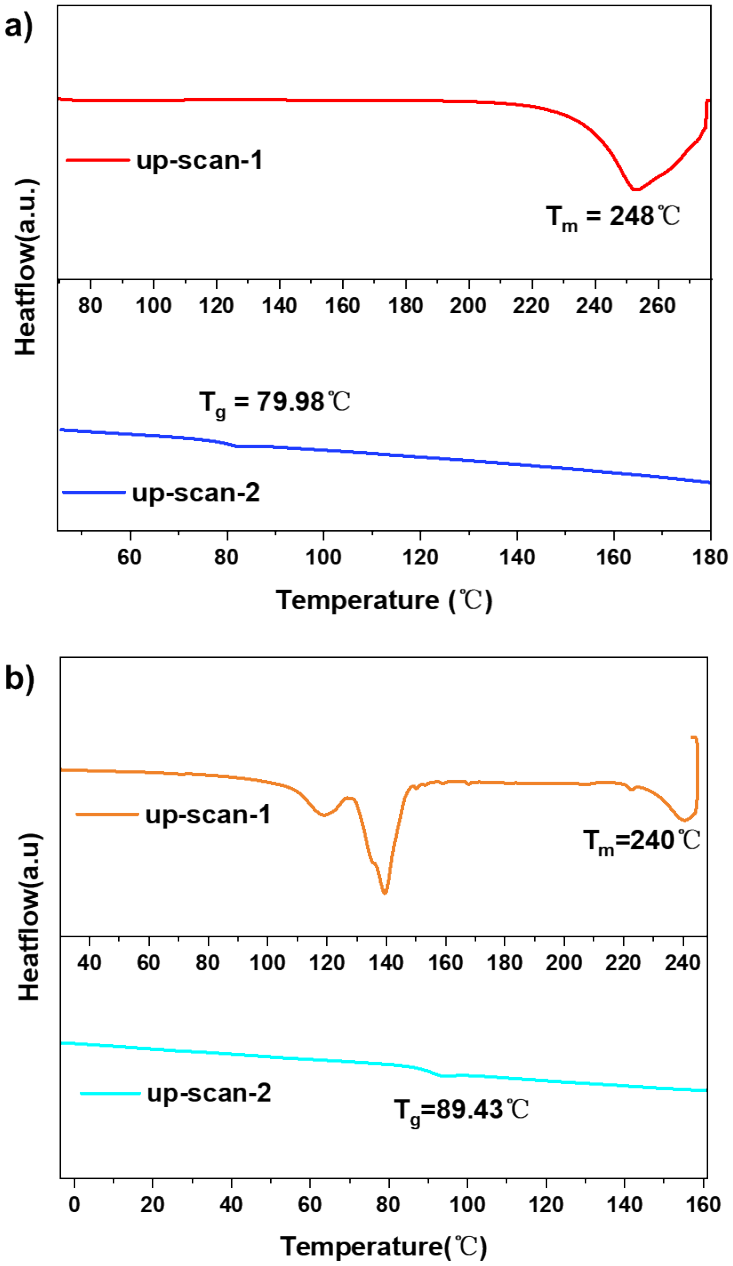

Fig. S5 DSC diagrams of a) AC1 and b) AC2.

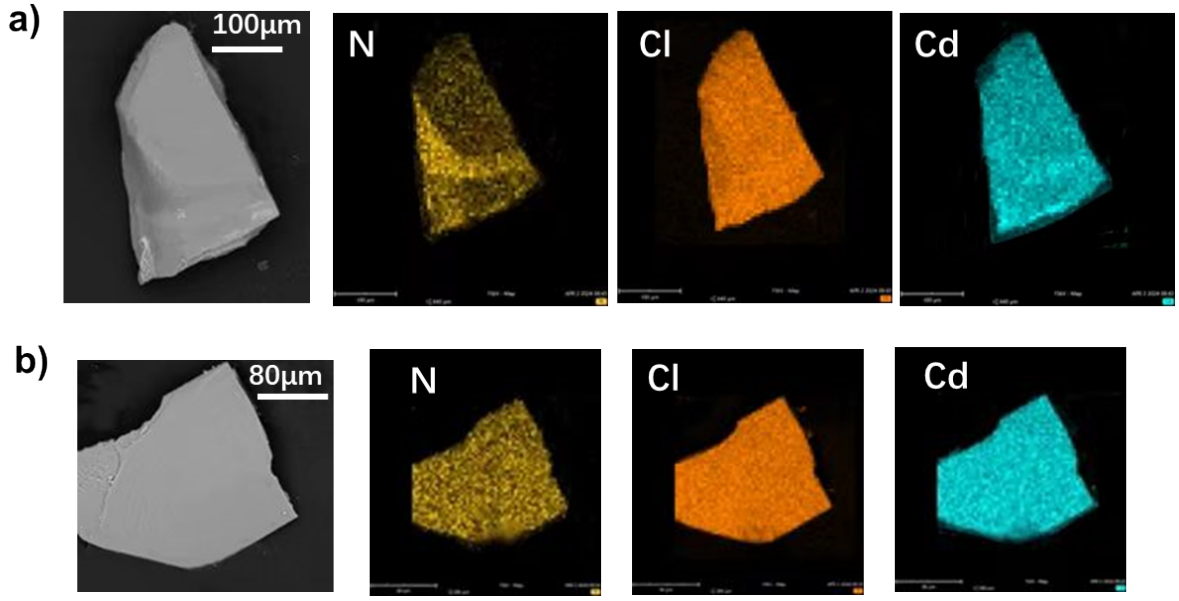

Fig. S6 EDS images of a) AC1 and b) AC2 .

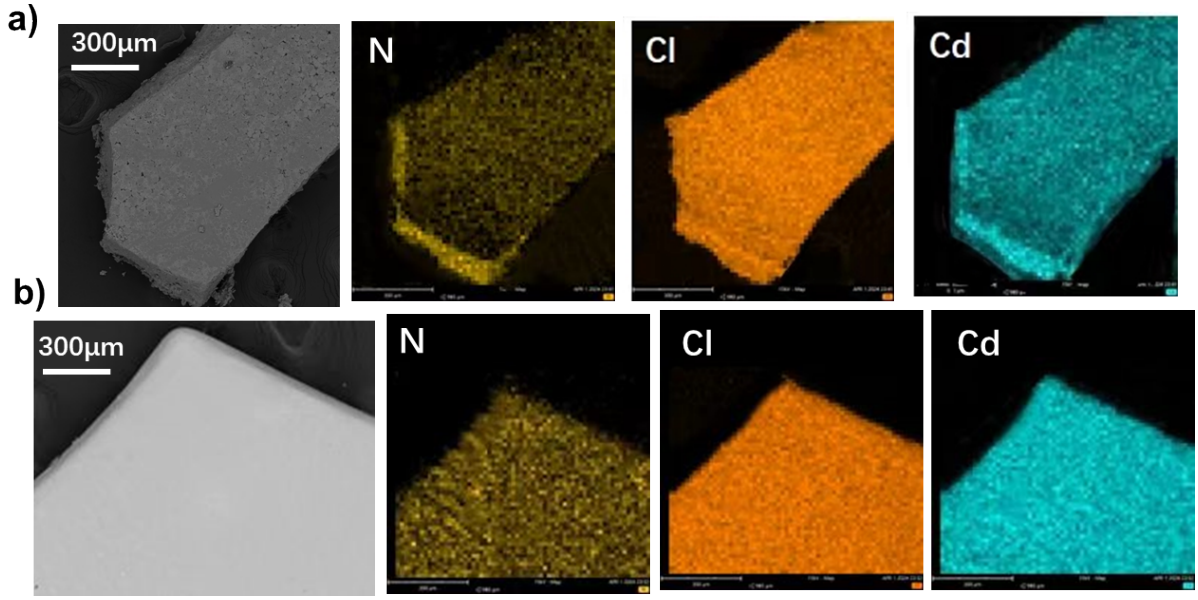

Fig. S7 EDS images of a) AC1-A and b) AC2-A .

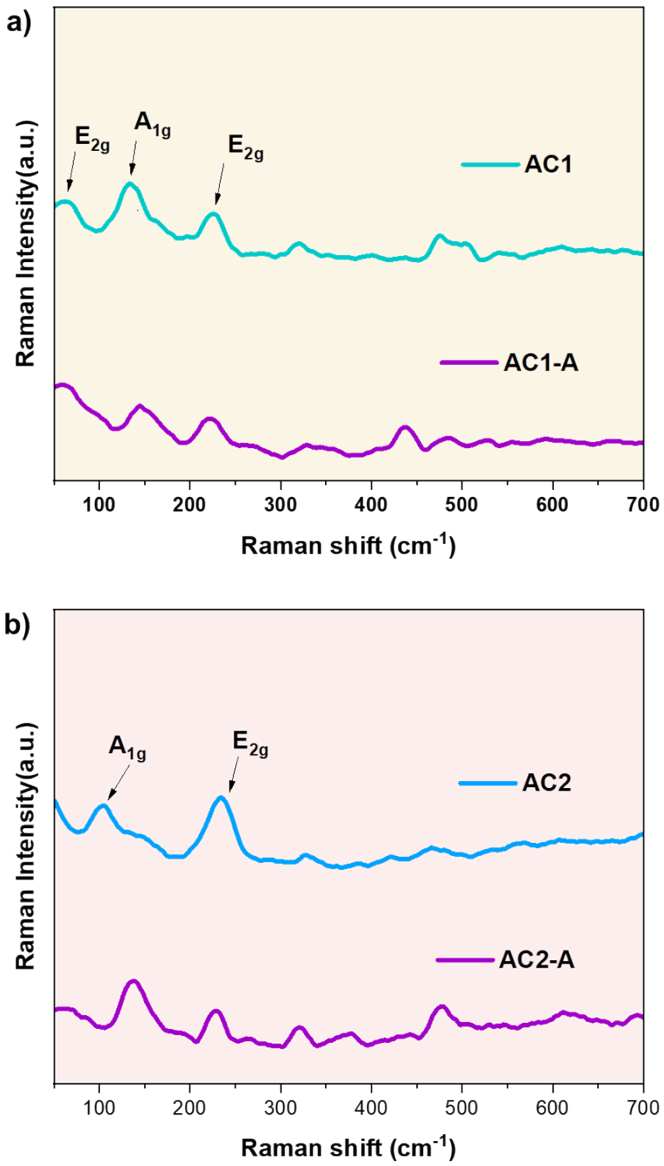

Fig. S8 Raman spectra of a) AC1 and AC1-A, b) AC2 and AC2-A.

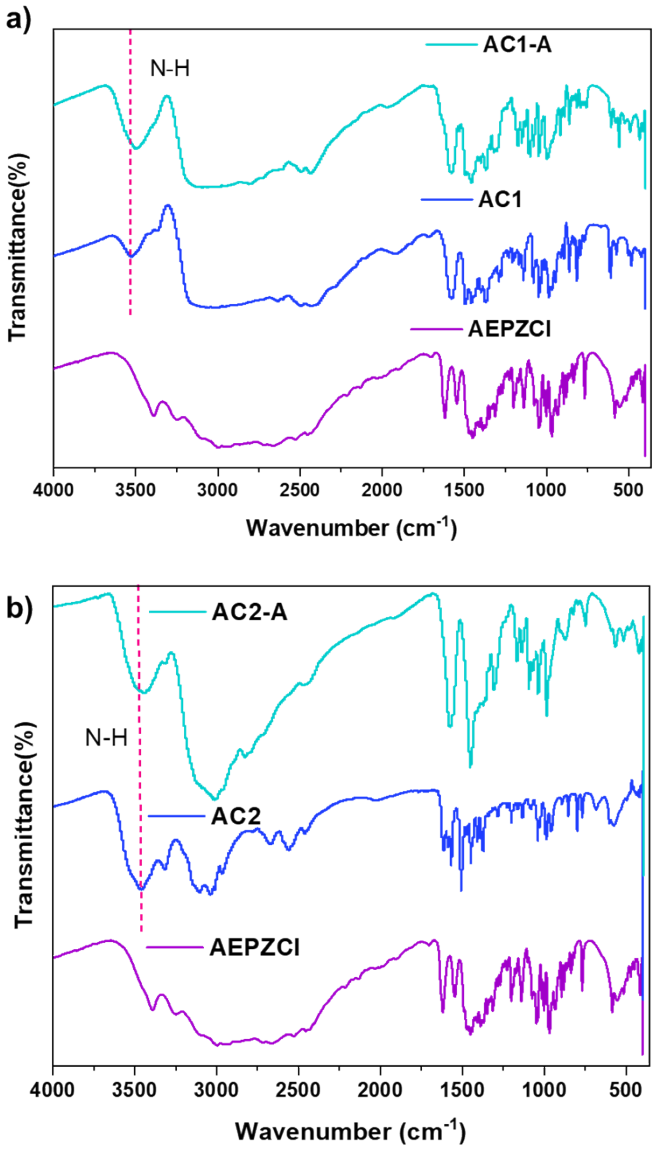

Fig. S9 Comparison in FTIR infrared spectra of a) AC1-A and AC1, b) AC2-A and AC2.

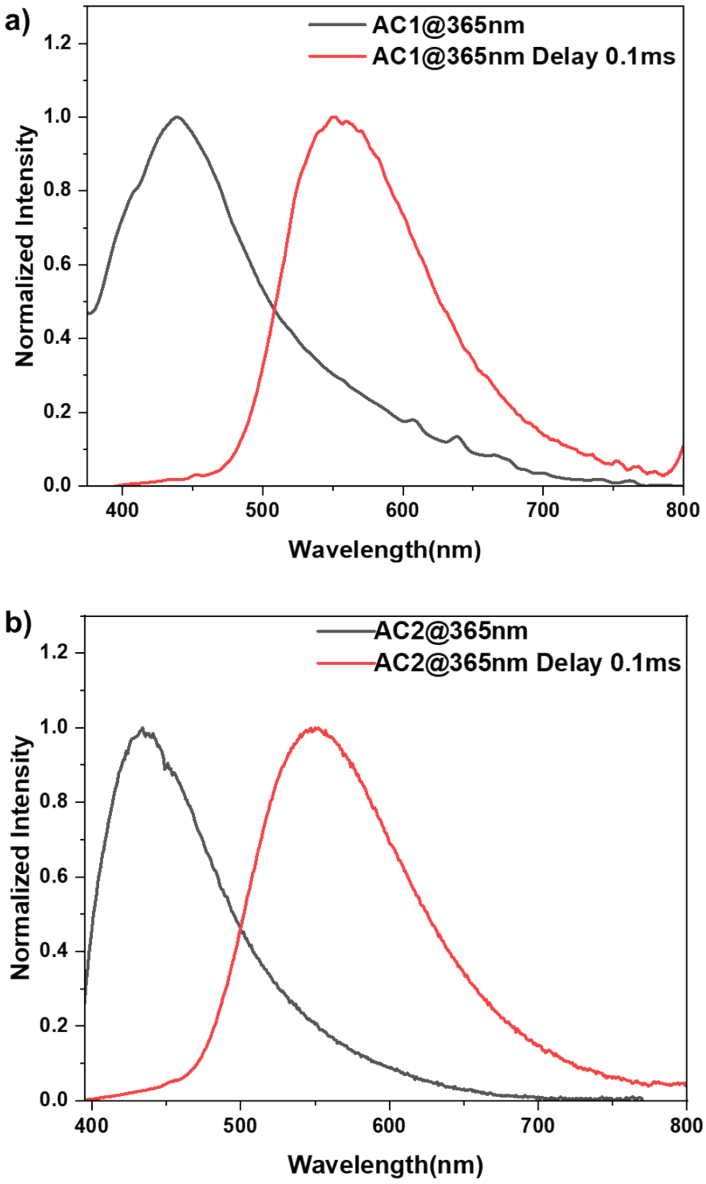

Fig. S10 Prompt and delayed (t_d = 0.1 ms) emission spectra of a) AC1 and b) AC2 (λ_{ex} = 365 nm).

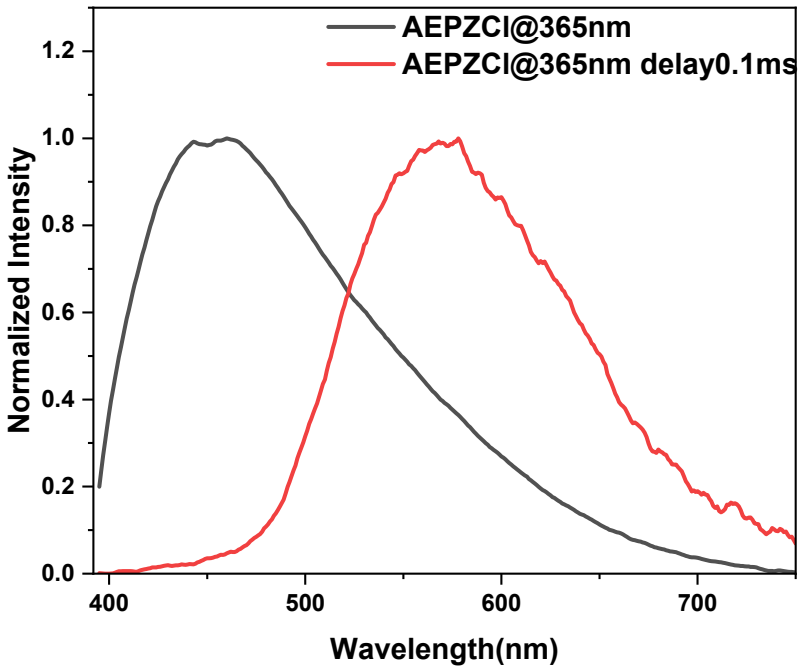

Fig. S11 The steady-state and delayed 0.1 ms emission spectrum of AEPZCl (λ_{ex} = 365 nm).

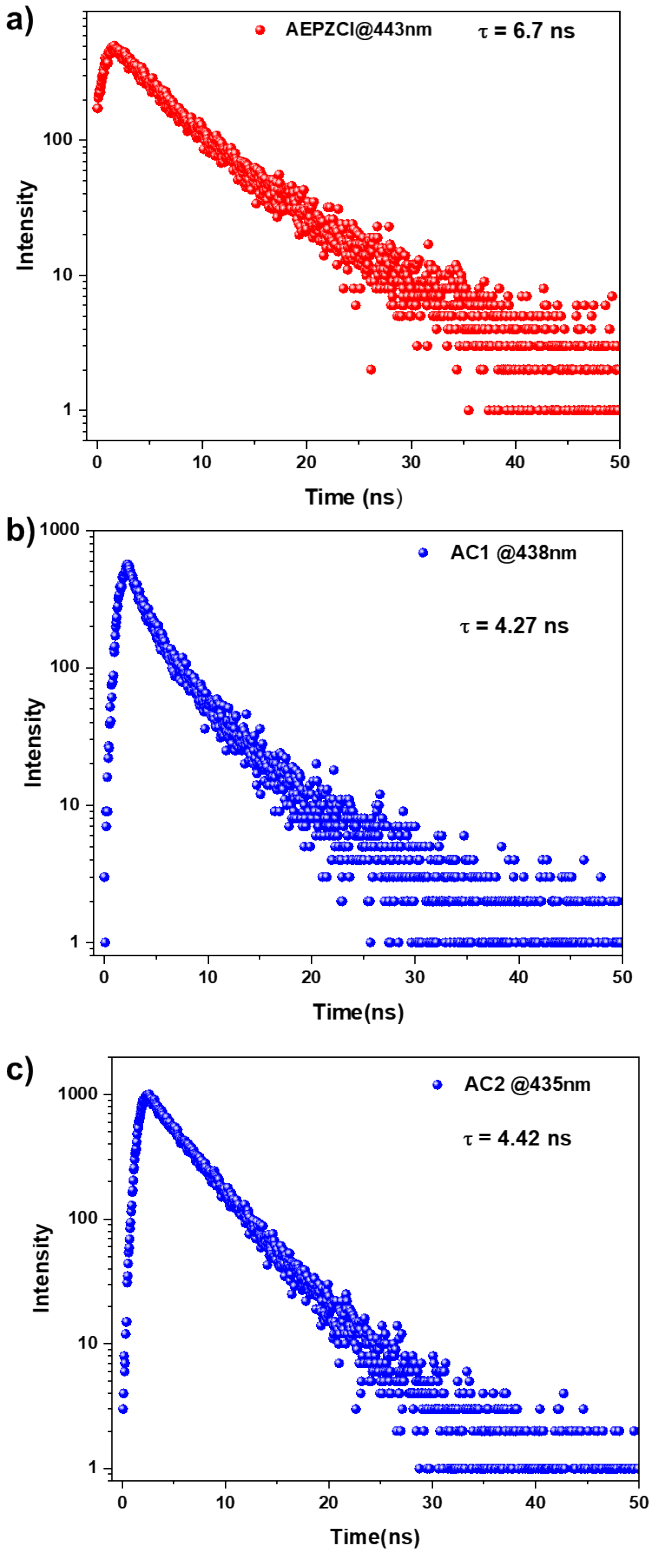

Fig. S12 Transient luminescence decay curves of a) AEPZCl, b) AC1 and c) AC2 monitored at 443 nm, 438 nm and 435 nm, respectively.

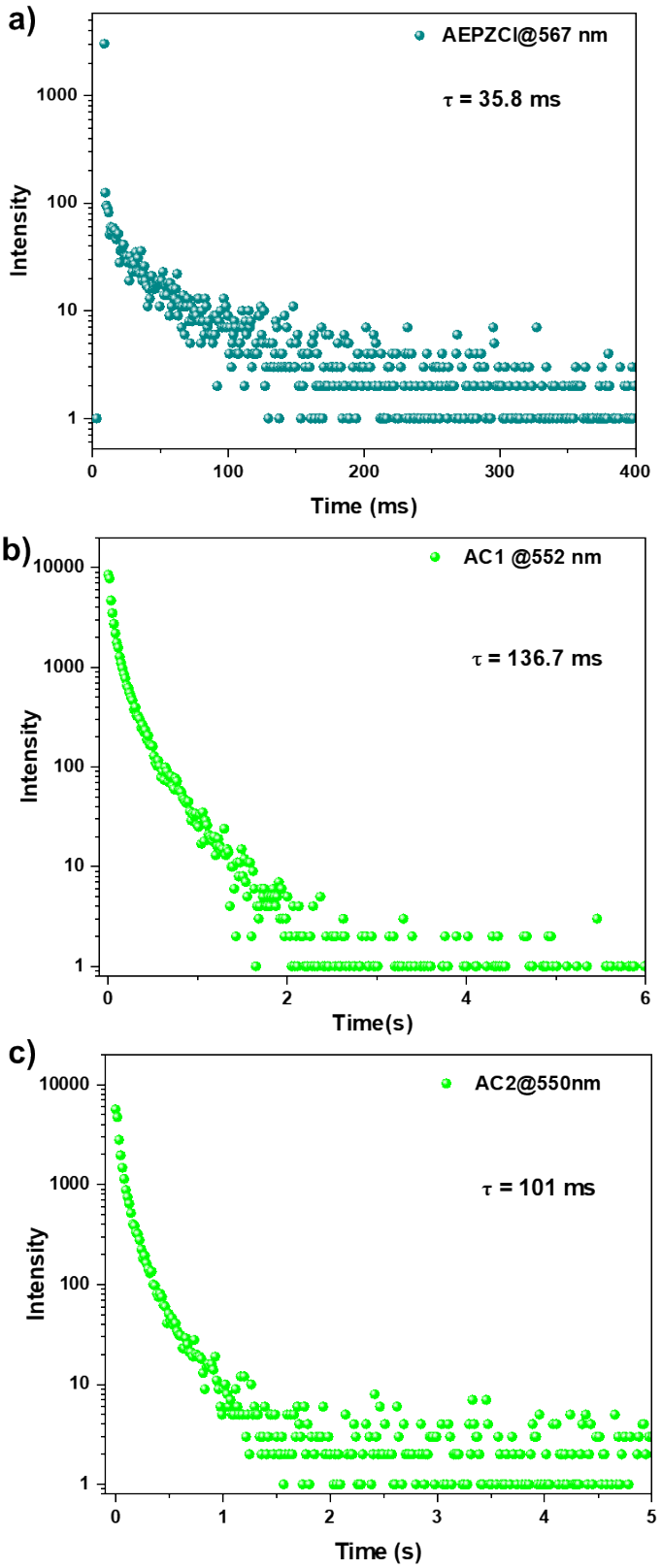

Fig. S13 Transient luminescence decays of a) AEPZCl, b) AC1 and c) AC2 monitored at 567 nm, 552 nm and 550 nm, respectively.

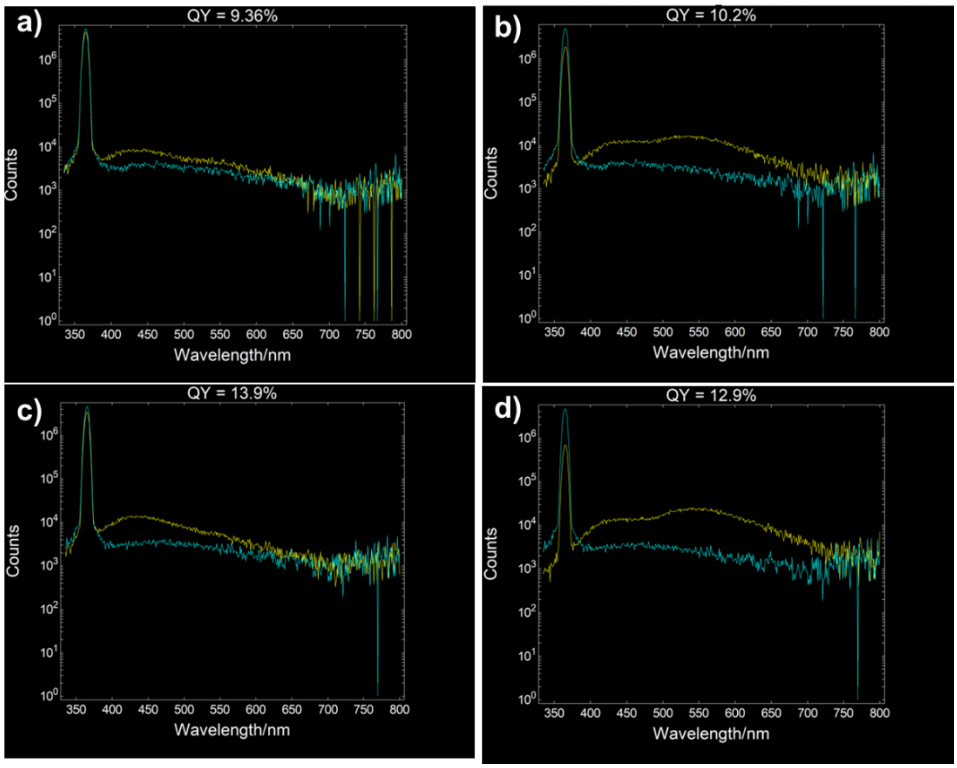

Fig. S14 Quantum yield of a) AC1, b) AC1-A, c) AC2, d) AC2-A (λ_{ex} = 365 nm).

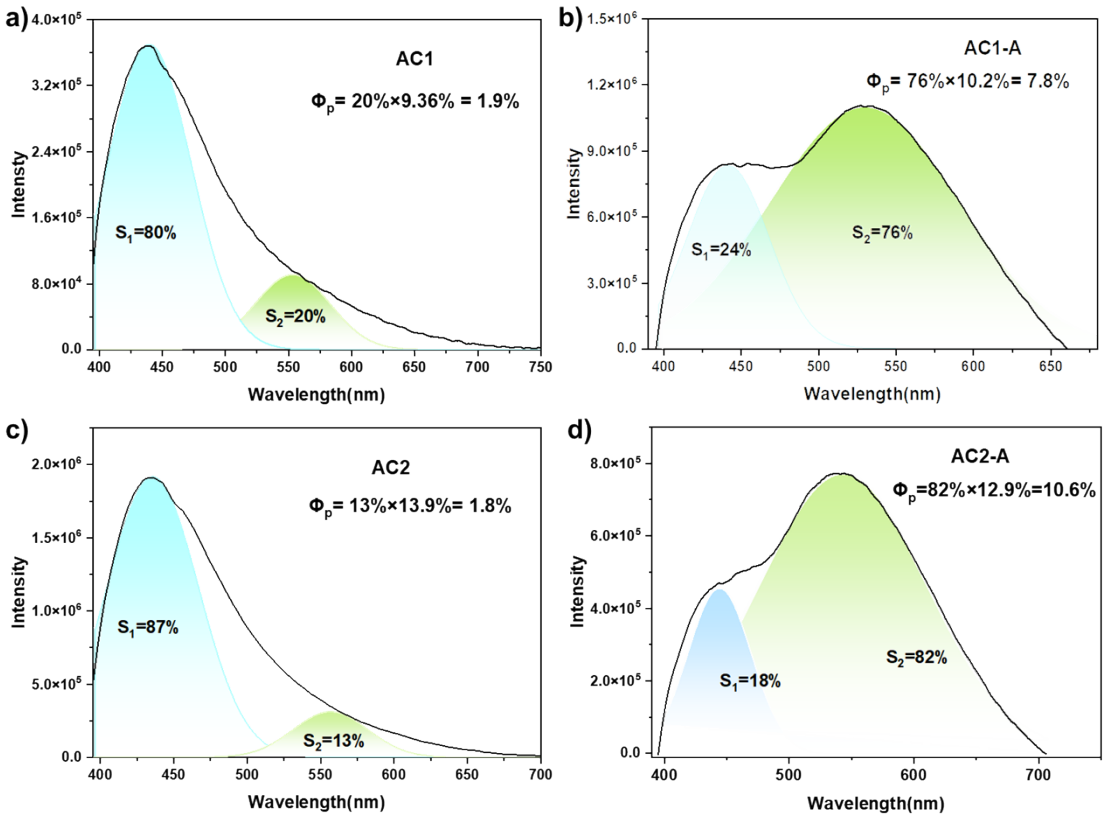

Fig. S15 Gaussian fitting of PLQY results of a) AC1, b) AC1-A, c) AC2, d) AC2-A with emission peaks of 445 nm and 550 nm (λ_{ex} = 365 nm).

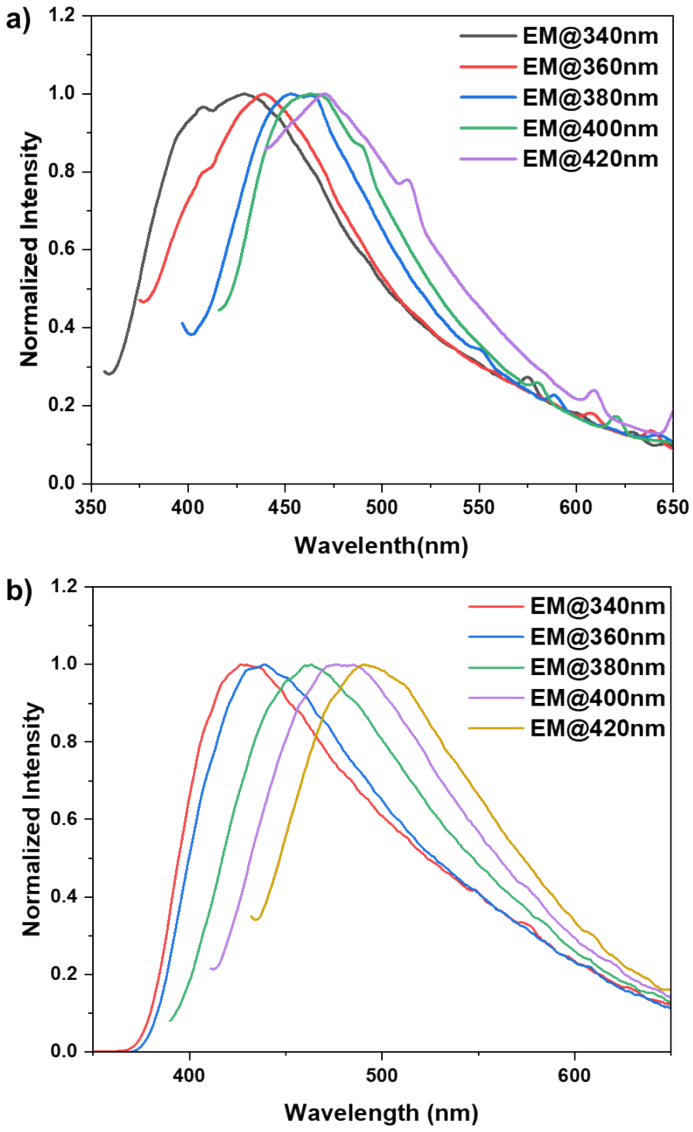

Fig. S16 Emission spectra of a) AC1 and b) AC2 recorded at different excitation wavelengths.

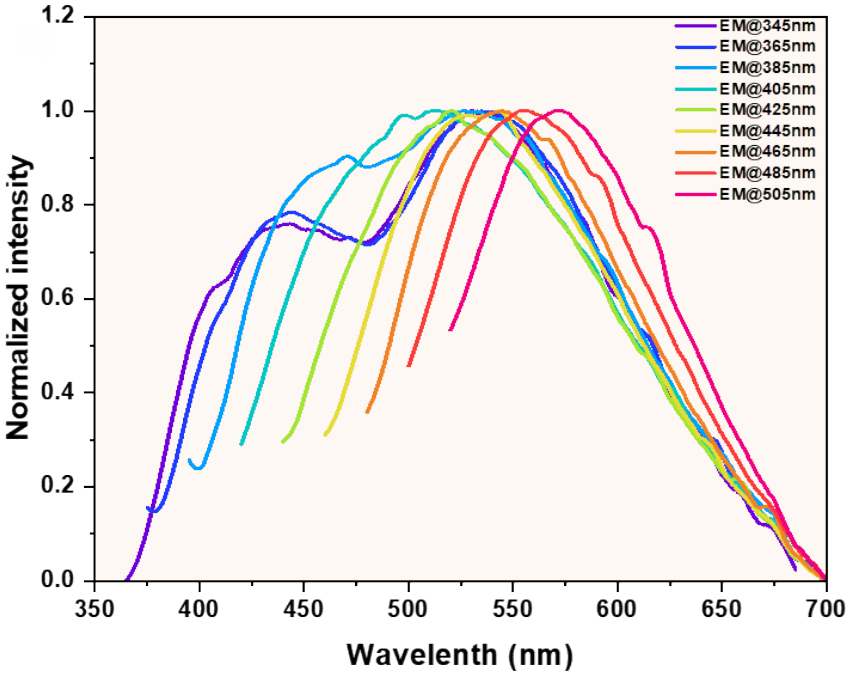

Fig. S17 Emission spectra of AC1-A recorded at different excitation wavelengths.

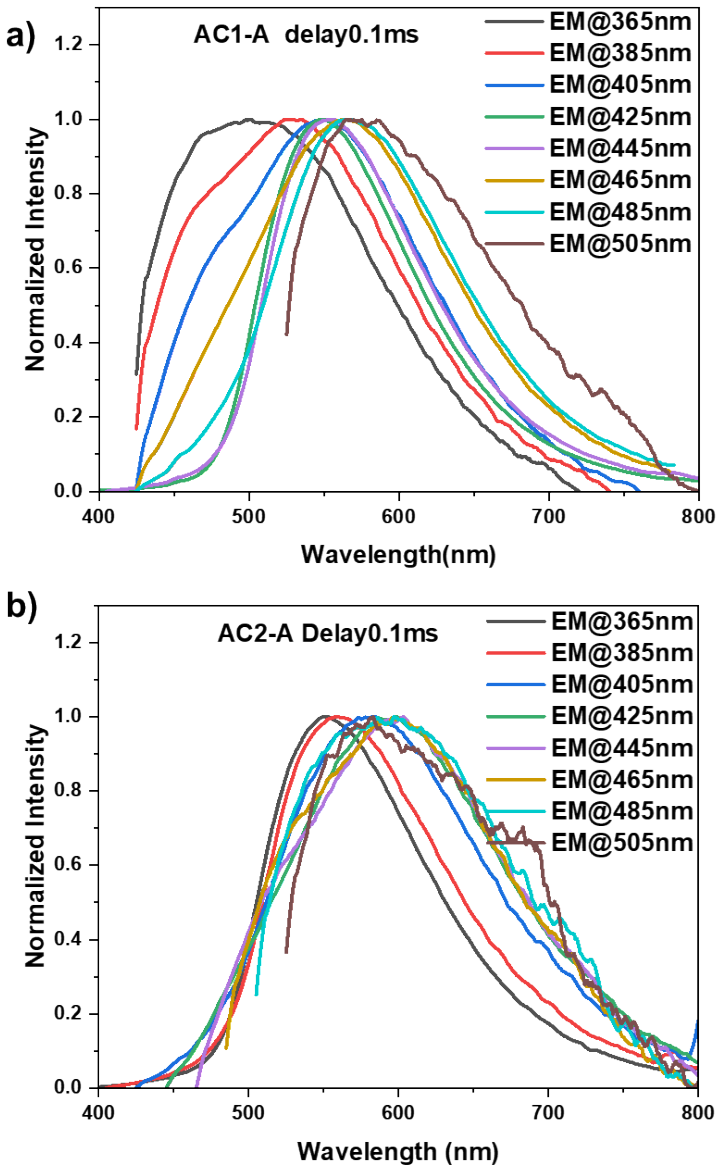

Fig. S18 Delay emission spectra of AC1-A (a) and AC2-A (b) recorded at different excitation wavelengths.

Table S2 Related photophysical parameters of AEPZCl, AC1, AC2, AC1-A, AC2-A, AC3-A and AC4-A.

	Prompt			Delay		
Compound	λ_{ex}（nm）	λ_{em}（nm）	τ（ns）	λ_{ex}（nm）	λ_{em}（nm）	τ（ms）
AEPZCl	365	443	6.7	365	567	35.8
AC1	365	438	4.27	365	552	136.7
AC2	365	435	4.42	365	550	101
AC1-A	365	444 532	/	365	548	310
AC2-A	365	444 541	/	365	551	419
AC3-A	365	447 541 620	/	365	620	115.13
AC4-A	365	447 531 620	/	365	540 642	158.35 12.41

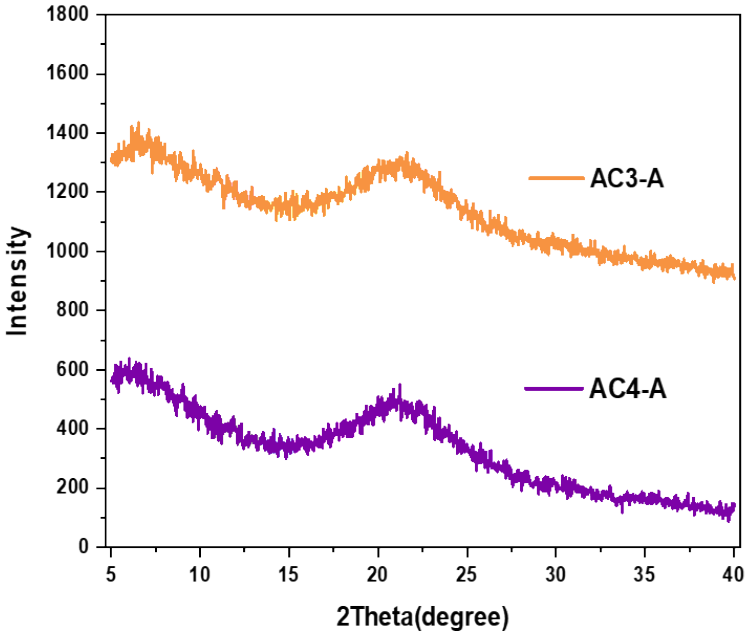

Fig. S19 PXRD patterns of AC3-A and AC4-A.

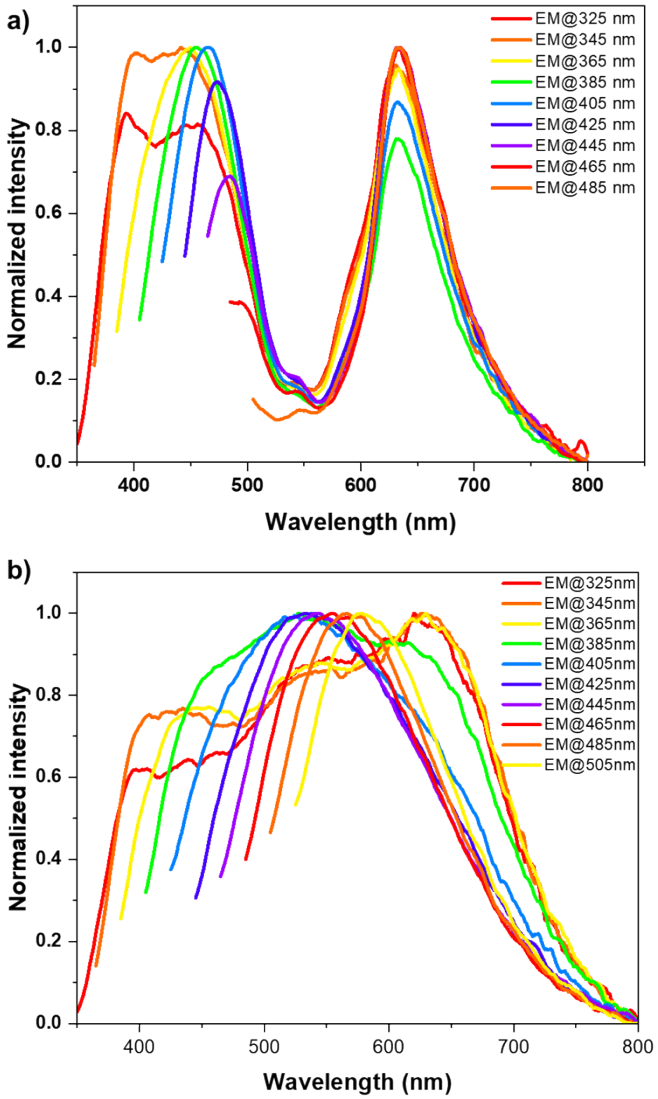

Fig. S20 Emission spectra of a) AC3-A and b) AC4-A recorded at different excitation wavelengths.

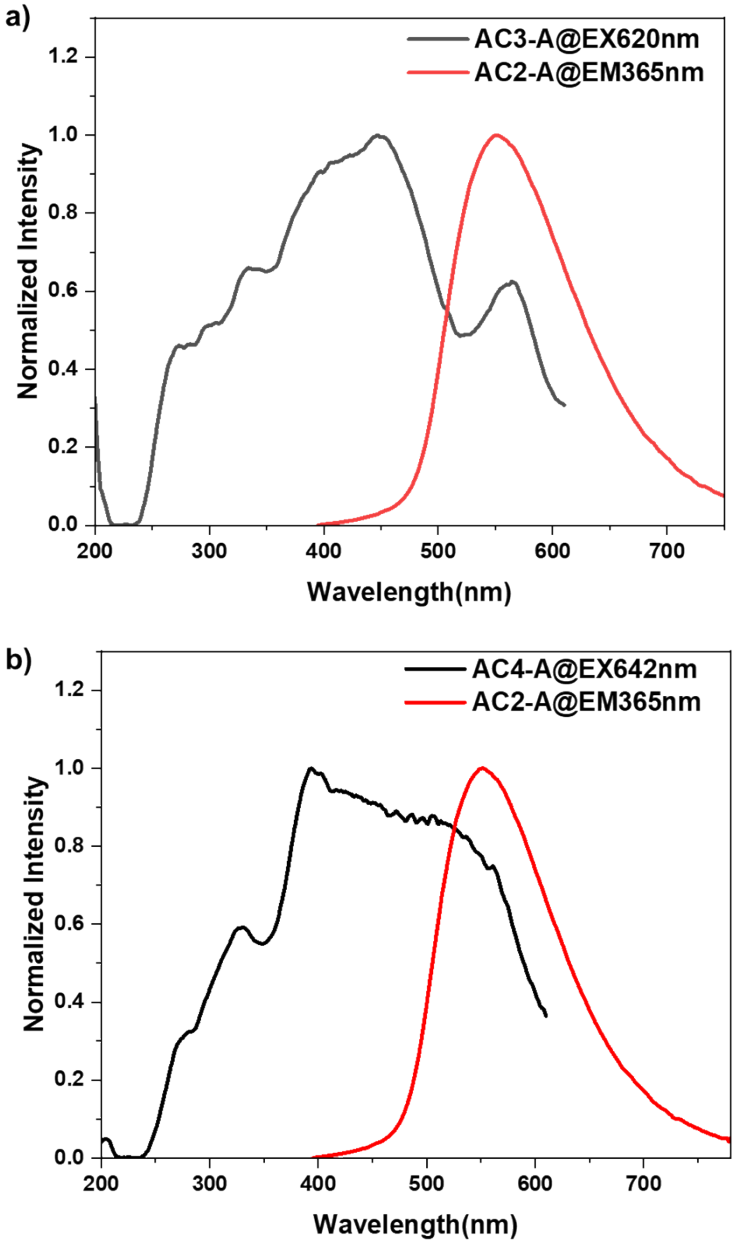

Fig. S21 a) Excitated spectra of AC3-A monitored at 620 nm and delayed emission spectra of AC2-A monitored at 365 nm. b) Excitated spectra of AC4-A at 642 nm and the delayed emission spectrum of AC2-A at 365nm.

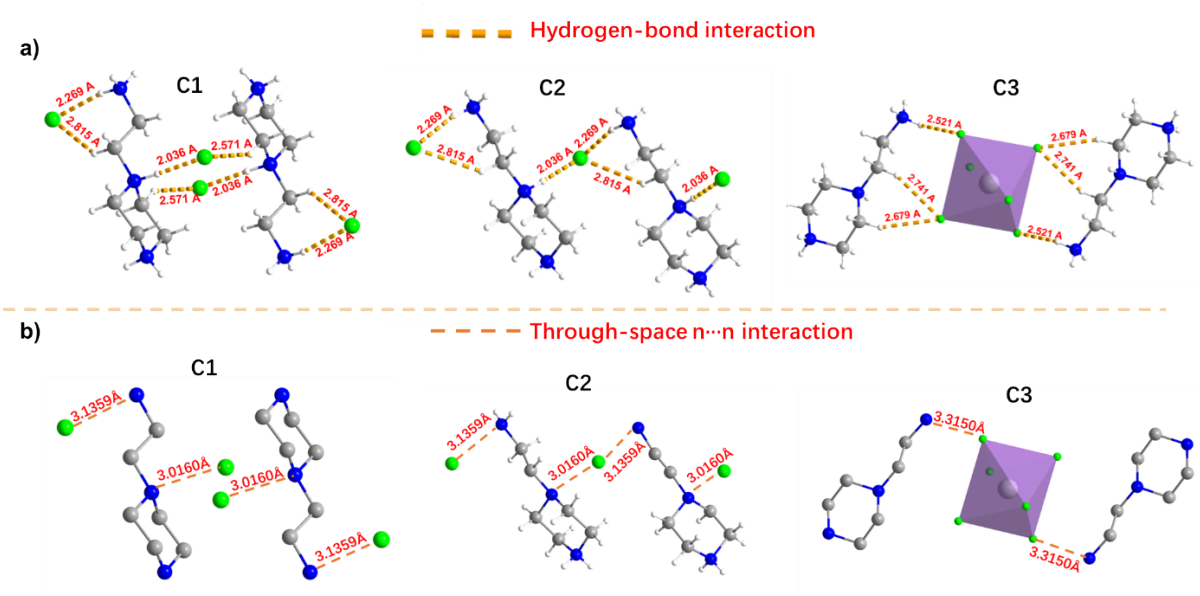

Fig. S22 a) Hydrogen bond interaction and b) n•••n interaction in cluster structure.

Table S3 Density values of AC1, AC1-A, AC2 and AC2-A.

	m (mg)	**V (cm^3)**	**P (mg/cm^3)**
AC1	\	\	1.757 [a]
AC1-A	0.2657	0.1	2.657
AC2	\	\	2.179 [a]
AC2-A	0.3786	0.1	3.786

[a] The density are derived from SCXRD date.

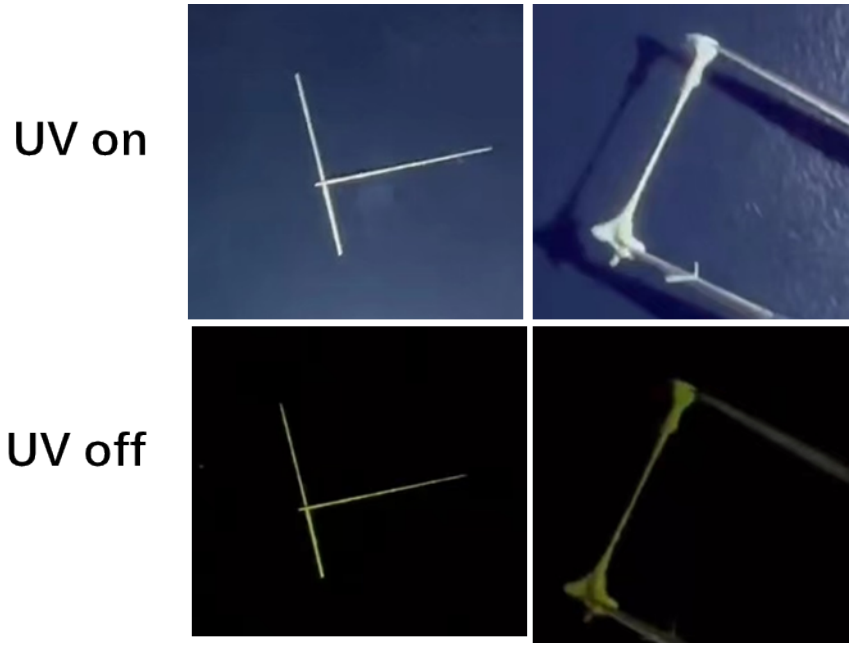

Fig. S23 Photos of AC2-A filament before and after UV light turned off.

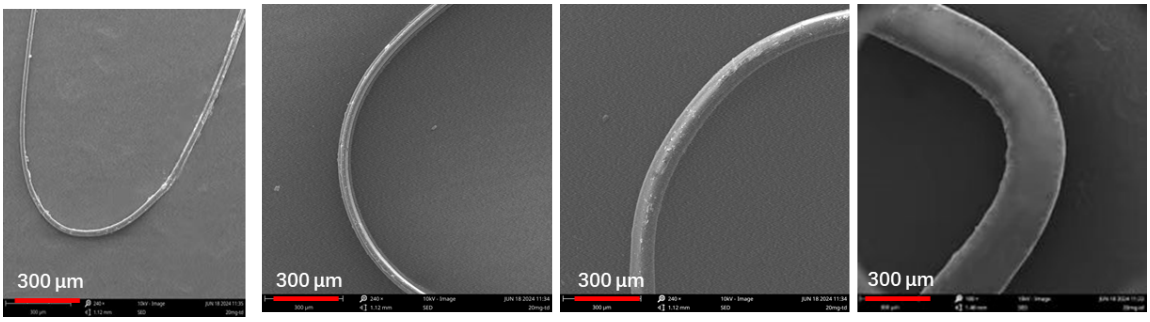

Fig. S24 SEM of bending A4C-A@PLA with different diameters.

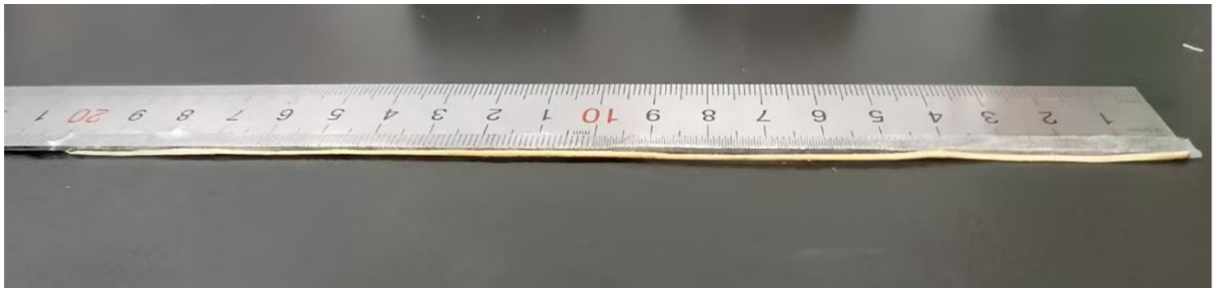

Fig. S25 Length of AC2-A@PLA.

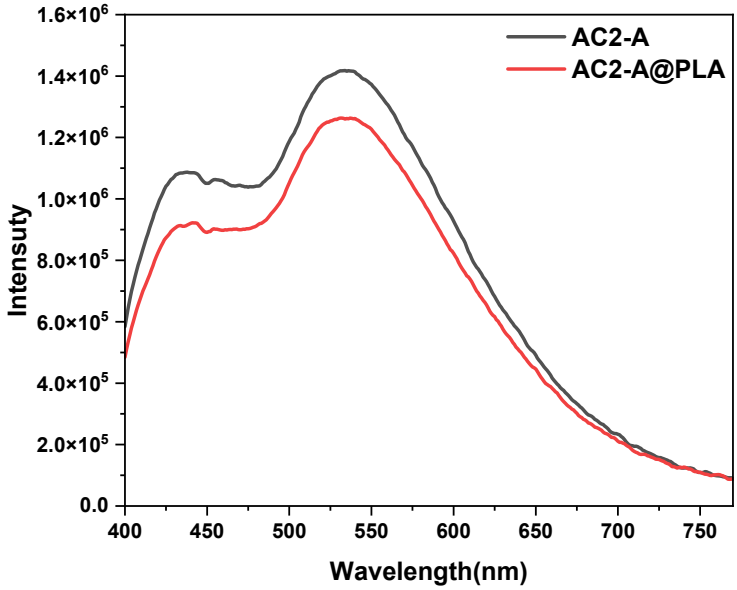

Fig. S26 Comparison of emission spectra between AC2-A@PLA and AC2-A.

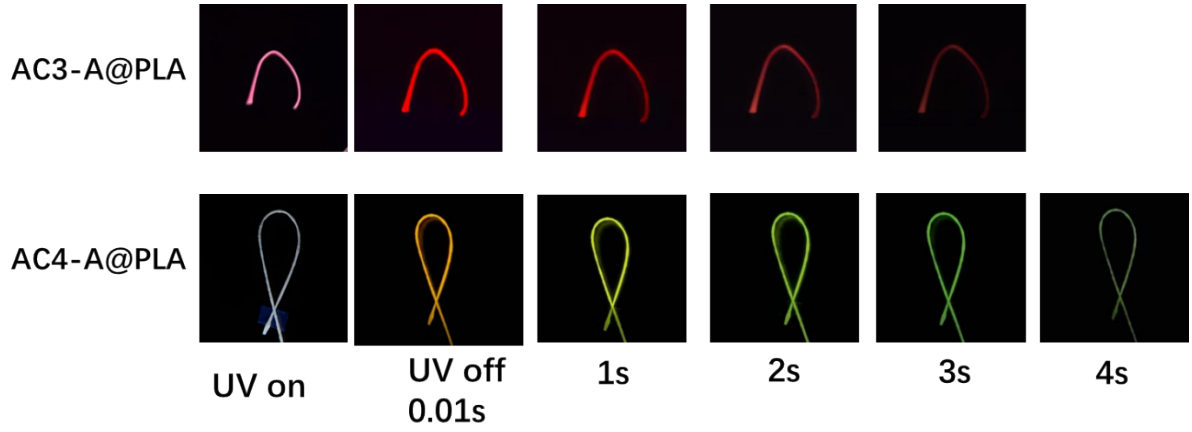

Fig. S27 Photos of composite materials AC3-A@PLA and AC4-A@PLA before and after UV light turned off.

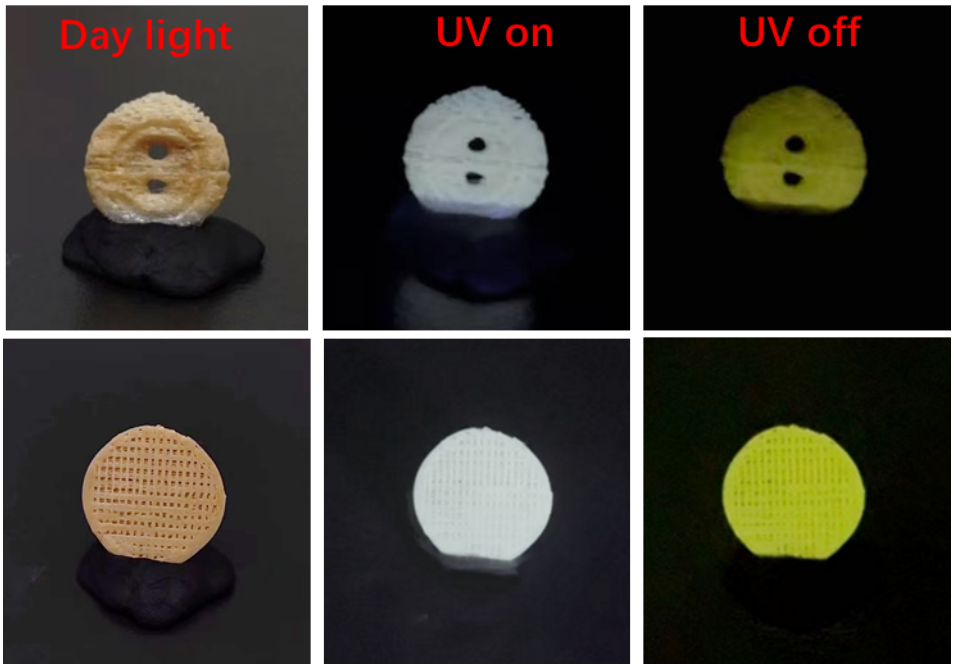

Fig. S28 Photos of 3D printed frameworks of AC2-A@PLA under UV on and off.

Table S4 Corresponding values of Morse code and letters.

Code	Character	Code	Character
• – • •	**L**	– •	**N**
• • • –	**V**	• –	**A**
• • – •	**F**	– •	**N**
– • – –	**Y**	• – •	**R**
– – • –	**Q**	– • •	**D**
• – – –	**J**	• • –	**U**

Reference

1. Z. Liu, T. Lu and Q. Chen, An sp-hybridized all-carboatomic ring, cyclo[18]carbon: Electronic structure, electronic spectrum, and optical nonlinearity, *Carbon*, 2020, **165**, 461-467.